The Experimental Study for the Influence of Bed Diameter and Bed Height on Dryout Heat Flux (DHF) using a Non-Heating Methodology

Je-Young Moon and Bum-Jin Chung*
Department of Nuclear Engineering, Kyung Hee University
#1732 Deogyeong-daero, Giheung-gu, Yongin-si, Gyeonggi-do, 17104, Korea
**Corresponding author: bjchung@khu.ac.kr*

1. Introduction

For an ex-vessel scenario of molten corium by the reactor pressure vessel (RPV) failure, the jet break-up, droplet solidification and debris bed settling occur in sequence (Fig. 1). The relocated debris beds may cause the molten core-concrete interaction (MCCI) [1-6]. In order to prevent the MCCI, it is important to evaluate the coolability of ex-vessel debris beds. The vaporization of water removes the decay heat of debris beds. Thus, the dryout heat flux (DHF) is defined as the maximum heat removal rate of debris beds [7-13]. It is essential to investigate the influence of parameters (bed diameter, bed height, flooding condition, etc.) on the coolability of debris beds.

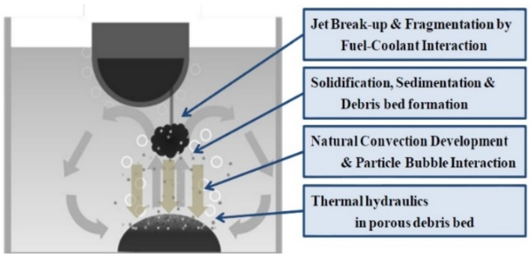

Fig. 1. A development process of corium debris bed in the flooded cavity pool [6].

In this study, the dryout heat flux (DHF) of debris beds was measured by mass transfer experimental methodology. The conventional copper electroplating system using $CuSO_4$-H_2SO_4, was extended to boiling heat transfer using the hydrogen generated at the cathode surface at a high potential. This non-heating method of DHF measurement simulates the uniform self-heating condition of debris beds. For the bottom flooding condition, the bed diameter and bed height were 3 mm to 6 mm and 20 mm to 60 mm, respectively. The copper or stainless steel cathode acted as the volumetrically heated debris beds. The experimental apparatus was the polycarbonate pipe filled with the cathode beds and the aqueous solution of the sulfuric acid (H_2SO_4).

2. Previous studies

The existing studies reported that the debris coolability is affected by the bed diameter, bed height, porosity, system pressure, flooding and coolant conditions, etc. Particularly, the DHF depends on the bed diameter, bed height and flooding condition.

The influence of the DHF on bed diameter and bed height was experimentally studied by Barleon *et al.* [8]. For top flooding condition, the bed diameter and bed height were varied 0.06 to 16 mm and 6 to 40 cm, respectively. The water or Freon-113 was used as the coolant. They reported the DHF increased with the bed diameter and decreased with the bed height regardless of coolant [14].

Hofmann [15] also performed the DHF experiment for top flooding and bottom flooding condition. The bed height varied up to 0.5 m and consisted of 3 mm stainless steel particles. The water was used as the coolant. The DHF for bottom flooding condition was more than twice as high as that from top flooding condition. The similar results for the flooding condition were reported by Atkhen and Berthoud [3], Rashid *et al.* [11], Squarer and Peoples [18], and Kulkarni *et al.* [19].

Afterward, Hofmann [16] confirmed the influence of the bed diameter and height on the DHF for the top flooding condition. The uniform beds consisted of stainless steel balls of 1 and 3 mm in diameter up to 100 cm height. They mentioned that the DHF decreased with increasing bed height. Dhir and Catton [17] also reported the similar result. Yamano *et al.* [1], Kim *et al.* [6], Bang and Kim [12], Hofmann [16], Squarer and Peoples [18] also confirmed the dryout heat density was improved by the bed diameter.

Although there have been considerable studies on the DHF of the debris beds either experimentally or theoretically, the range of parameters (bed diameter, bed height, porosity, etc.) was scattered due to uncertainty about the formation and settling of debris bed. Thus, it is difficult to compare the results of the existing studies.

3. Experiments

3.1 Analogy concept with the electroplating system

Heat and mass transfer systems are analogous, as the governing equations and parameters are of the same form mathematically [20, 21]. The experimental method using a copper sulfate-sulfuric acid ($CuSO_4$-H_2SO_4) electroplating system based on the analogy concept is well-established [22-28].

The copper sulfate-sulfuric acid ($CuSO_4$-H_2SO_4) electroplating system was generally used for analogy experiments for simulating single phase heat transfer system. This system is composed of the copper anode and the copper cathode submerged in an aqueous solution ($CuSO_4$-H_2SO_4).

3.2 Extended mass transfer experimental methodology

When the applied potential between cathode and anode increases, the current increases initially and then reaches a plateau. The current at the plateau is called as the limiting current. When the potential increases further beyond the limiting current region, the hydrogen ions reduce and the current increases again. It causes the evolution of hydrogen gas at the cathode.

In this study, the basic idea is that the vaporization can be simulated by the hydrogen gas generated at the cathode surface. The hydrogen film covering the cathode surface can be formed and the DHF condition in the heat transfer can be simulated [29]. When the electric potential is applied between the cathodes and anode, all the cathode beds of copper and stainless steel have the same potential difference, which means that a uniformly heating condition can be simulated.

Based on the assumption as mentioned above, the authors hypothesized that hydraulic behavior of gas over the arbitrary solid surface will be similar under the identical gaseous volume generation rate (η). Thus, the DHF can be calculated with Eq. (1) introducing the gas generation rate (η).

$$q_{DHF} = \eta h_{lg} \rho_g \quad (1)$$

The hydrogen generation rate (η) is determined by the electric current, charges for hydrogen reduction and Avogadro number (Eq. (2)).

$$\eta = V_m \left(\frac{T}{273.15}\right)\left(\frac{I}{neN_A}\right) \quad (2)$$

3.3 Experimental apparatus

Figure 2 shows the electric circuit of the experimental apparatus consisted of a polycarbonate pipe containing the cathode beds and anode, a power supply and a data acquisition system. The inner diameter and length of cathode part pipe are 46 mm and 815 mm. respectively. The diameter of copper and stainless steel beds is 3 to 6 mm. The height of beds is ranged from 20 to 60 mm. The test section is filled with the sulfuric acid solution (H_2SO_4) of 1.5 M. For the bottom flooding condition, the top and bottom of bed were open and the copper cathode beds were rested on a permeable support grid. The porosities of beds are 0.374 to 0.435 for all cases. The copper anode of 35 mm × 35 mm × 100 mm are placed at the lower part of the pipe to supply the electric charges. The power supply was used to apply current and data acquisition system was employed to record the experimental results. As the polycarbonate pipe was transparency, we can observe the behaviors of hydrogen vapor.

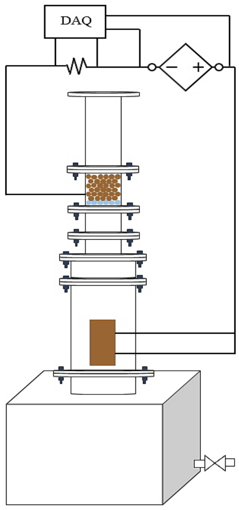

Fig. 2. The electric circuit of experimental apparatus.

4. Results and discussion

Figure 3 shows the measured currents depending on the applied potentials. The electric potential and the current correspond to the temperature difference and the heat flux in the heat transfer system, respectively. A step increase of the electric potential is made until a sudden drops of the current were observed. For copper beds of d=6 mm and H_d=60 mm, the sudden drops of the current were observed at the potential of 90 V and the current of 50 A. For high power, the pressure developed by the generated hydrogen gas retards the inflow of the sulfuric acid (H_2SO_4) solution into the copper cathode beds. The flow of the electric current is blocked by the hydrogen gas. It is similar to the dryout mechanism of heat transfer system. For other cases, the same mechanism was observed.

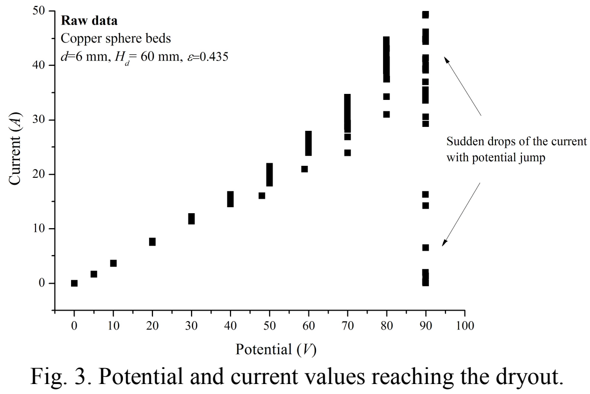

Fig. 3. Potential and current values reaching the dryout.

Figure 4 indicates the measured current and potential at the stabilized conditions. Almost linear increase of current with the potential was observed to reach the dryout condition. As a result, the calculated DHF by using Eq. (1) and (2) was 7.03 kW/m^2. For the decrease of bed diameter, the DHF of this study decreased up to 2 times. It is similar trend with the existing studies [6, 12, 16, 18, 30]. The DHF of the existing studies for the bottom flooding condition are summarized in Table Ⅰ.

The result of this study is maximum 300 times smaller than those of existing heat transfer studies. This discrepancy seems to be due to the differences in the physical parameters influencing the boiling mechanism. A plausible explanation for the discrepancy of the results is that the bottom flooding condition wasn't fully simulated because the captured hydrogen bubbles were observed at the underneath of the permeable support grid. As the captured bubbles obstructed the inflow of the sulfuric acid solution, the dryout condition was reached early. In addition, it was possible that the electric resistance of cathode beds had increased as the smaller hydrogen bubble and too many nucleation site caused the decrease of bed surface. In further studies, these are to be improved through some parametric corrections and design upgrade of test apparatus.

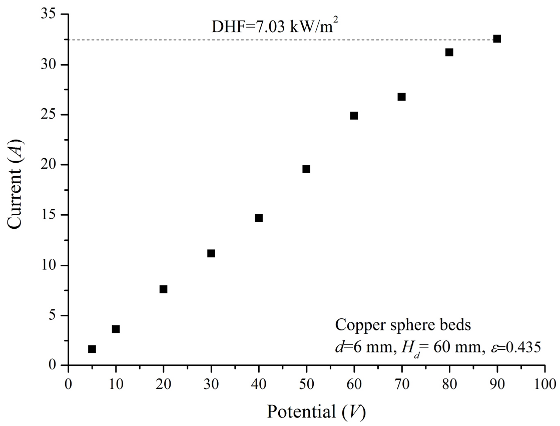

Fig. 4. Average potential and current values at equilibrium state reaching the dryout for the copper beds of H_d=60 mm.

Table Ⅰ: The DHF of the existing studies.

Authors	***d* (mm)**	***H_d* (m)**	***ε***	**DHF (kW/m^2)**
Hu and Theofanous [7]	7-9	1.02	-	612
Barleon *et al.* [8]	2	0.2	0.373	630
Bang and Kim [12]	3.2, 4.8	0.3	0.37, 0.38	900-1,200
Hofmann [15]	3	0.485	0.405	2,200
Cha and Chung [30]	1.5-4	0.11	-	900-1,800

Figure 5 shows the DHF according to the bed height (H_d) of copper and stainless steel beds for the bottom flooding condition. The bed height was varied from 20 to 60 mm. The DHF decreases with the bed height regardless of the cathode materials. This trend is similar to those of existing studies [3, 8, 15-18].

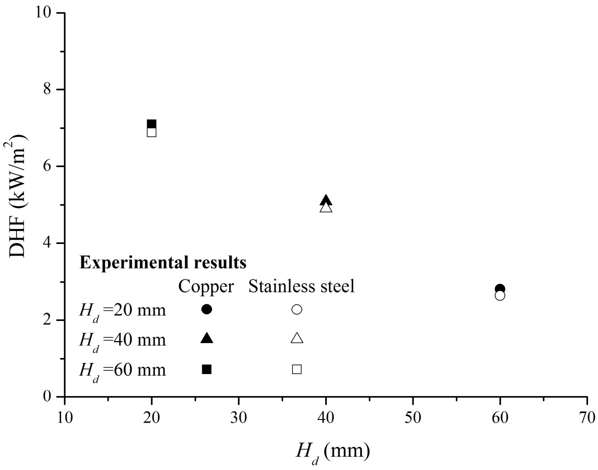

Fig. 5. Dryout heat flux according to the bed height (H_d) of copper and stainless steel beds.

5. Conclusions

The dryout heat flux (DHF) was measured by the mass transfer system extended the conventional copper-sulfate electroplating system, which is composed of the sulfuric acid solution and the copper electrodes. This non-heating method of DHF measurement simulates the uniform self-heating condition of debris beds.

The DHF can be directly calculated by the measured electric current from the present work. The DHF was increased by the increase of the bed diameter and the decrease of the bed height regardless of the cathode materials. These tendency for the DHF is similar to that of existing studies. However, the measured DHF values had large discrepancy with those of the existing heat transfer studies. The discrepancy is natural due to the physical parameters influencing the boiling mechanism. Also, the obstruction of inflowing the sulfuric acid solution occurred as the hydrogen bubbles were captured at the underneath of the permeable support grid. Thus, we will perform the parametric corrections. The design of the experimental apparatus must be upgraded to eliminate the factors increasing the uncertainty of experimental data. Also, further studies such as the influence of the flooding condition must be performed to approach the heat transfer system.

ACKNOWLEDGEMENT

This study was sponsored by the Ministry of Science and ICT (MSIT) and was supported by Nuclear Research & Development program grant funded by the National Research Foundation (NRF) (Grant code: 2017M2A8A4056304).

REFERENCES

[1] N. Yamano *et al.*, TECHNICAL NOTE ON EX-VESSEL CORE MELT DEBRIS COOLABILITY AND STEAM EXPLOSIONS, NEA/CSNI/R(96)24, 1996.

[2] Y. Maruyama *et al.*, RECENT RESULTS OF MCCI STUDIES IN COTELS PROJECT, Third Korea-Japan Symposium on Nuclear Thermal Hydraulics and Safety (NTHAS3), Gyeongju, Korea, Oct. 13-16, 2002.

[3] K. Atkhen, G. Berthoud, SILFIDE experiment: Coolability in a volumetrically heated debris bed, Nuclear Engineering and Design, 236, 2126-2134, 2006.

[4] H.J. Allelein, M. Bürger, Considerations on ex-vessel corium behavior: Scenarios, MCCI and coolability, Nuclear Engineering and Design, 236, 2220-2236, 2006

[5] M.T. Farmer *et al.*, CORIUM COOLABILITY UNDER EX-VESSEL ACCIDENT CONDITIONS FOR LWRs, Nuclear Engineering and Technology, 41(5), 575-602, 2009.

[6] E.H. Kim *et al.*, Experimental Study on the Ex-Vessel Corium Debris Bed Development under Two-Phase Natural Convection Flows in Flooded Cavity Pool, The 7th European Review Meeting on Severe Accident Research (ERMSAR-2015), Marseille, France, Mar. 24-26, 2015.

[7] K. Hu, T.G. Theofanous, ON THE MEASUREMENT AND MECHANISM OF DRYOUT IN VOLUMETRICALLY HEATED COARSE PARTICLE BEDS, International Journal of Multiphase Flow, 17(4), 519-532, 1991.

[8] L. Barleon *et al.*, COOLING OF DEBRIS BEDS, Nuclear Technology, 65, 67-86, 1984.

[9] P. Schäfer *et al.*, Basic investigations on debris cooling, Nuclear Engineering and Design, 236, 2104-2116, 2006.

[10] E. Takasuo, An experimental study of the coolability of debris beds with geometry variations, Annals of Nuclear Energy, 92, 251-261, 2016.

[11] M. Rashid *et al.*, Experimental results on the coolability of a debris bed with multidimensional cooling effects, Nuclear Engineering and Design, 241, 4537-4543, 2011.

[12] K.H. Bang, J.M. Kim, ENHANCEMENT OF DRYOUT HEAT FLUX IN A DEBRIS BED BY FORCED COOLANT FLOW FROM BELOW, Nuclear Engineering and Technology, 42(3), 297-304, 2010.

[13] G. Repetto *et al.*, Investigation of Multidimensional Effects during Debris Cooling, The 5th European Review Meeting on Severe Accident Research (ERMSAR-2012), Cologne, Germany, mar. 21-23, 2012.

[14] R.J. Lipinski, A model for Boiling and Dryout in Particle beds, NUREG/CR-2646, 1982.

[15] G. Hofmann, ON THE LOCATION AND MECHANISMS OF DRYOUT IN TOP-FED AND BOTTOM-FED PARTICULATE BEDS, Nuclear Technology, 65, 36-45, 1984.

[16] G. Hofmann, DRYOUT IN VERY DEEP PARTICULATE BEDS, Nuclear Engineering and Design, 99, 177-185, 1987.

[17] V.K. Dhir, I. Catton, Dryout Heat Fluxes in Very Deep Debris Beds, Transactions of the American Nuclear Society, 35, 360-361, 1980.

[18] D. Squarer, J.A. Peoples, Dryout during Inductively-Heated Bed With and Without Forced Flow, Transactions of the American Nuclear Society, 34, 535-537, 1980.

[19] P.P. Kulkarni *et al.*, Experimental investigation of coolability behavior of irregularly shaped particulate debris bed, Nuclear Engineering and Design, 240, 3067-3077, 2010.

[20] A. Bejan, Convection Heat Transfer, fourth ed. Wiley & Sons, New Jersey, 2003.

[21] F.P. Incropera *et al.*, Principles of heat and mass transfer, 7th ed. John Wiley & Sons, INC., New York, 2013.

[22] E.J. Fenech, C.W. Tobias, Mass transfer by free convection at horizontal electrodes, Electrochimica Acta, 2, 311-325, 1960.

[23] J.R. Selman, C.W. Tobias, Mass-transfer measurement by the limiting-current technique, Advance in Chemical Engineering, 10, 211-318, 1978.

[24] C.W. Tobias, R.G. Hickman, Ionic mass transfer by combined free and forced convection, Zeitschrift für Physikalische Chemie-International Journal of Research in Physical Chemistry Chemical Physics, 229, 145-166, 1965.

[25] S.H. Ko *et al.*, Applications of electroplating method for heat transfer studies using analogy concept, Nuclear Engineering and Technology, 38, 251-258, 2006.

[26] J.H. Park *et al.*, Natural convection of an inclined helical coil in a duct, International Communications in Heat and Mass Transfer, 59, 11-16, 2014.

[27] H.K. Park, B.J. Chung, Mass Transfer Experiments for the Heat Load during In-Vessel Retention of Core Melt, Nuclear Engineering and Technology, 48, 906-914, 2016.

[28] D.Y. Lee *et al.*, Natural convective heat transfer of heated packed beds, International Communications in Heat and Mass Transfer, 88, 54-62, 2017.

[29] J. Krysa *et al.*, Free convection mass transfer in open upward-facing cylindrical cavities, Chemical Engineering Journal, 79, 179-186, 2000.

[30] J.H. Cha and M.K. Chung, Forced Flow Dryout Heat Flux in Heat Generating Debris Bed, Journal of Korean Nuclear Society, 18(4), 273-280, 1986.